

## Continuous Ferroelastic Phase Transition of a KBr:KCN Mixed Crystal

K. Knorr and A. Loidl

*Institut für Physik, D-6500 Mainz, Federal Republic of Germany*

and

J. K. Kjems

*Risø National Laboratory, Roskilde, Denmark*

(Received 24 July 1985)

The ferroelastic phase transition of  $(\text{KBr})_{0.27}(\text{KCN})_{0.73}$  has been studied by x-ray diffraction, ultrasonics, and inelastic neutron scattering. It is the first example of a cubic crystal where the elastic shear constant  $C_{44}$  softens completely corresponding to the  $m=2$  universality class.  $C_{44}$  and the Bragg intensities show a nonclassical critical behavior.

PACS numbers: 64.70.Kb, 61.12.Fy, 62.20.Dc

$(\text{KBr})_{1-x}(\text{KCN})_x$  mixed crystals have been studied intensively in the last years because they are conceptually simple examples of systems with a coupling of the phonon modes to the rotational degrees of freedom, here of the dumbbell-shaped CN ion. As a consequence of this coupling the CN-rich crystals ( $x > 0.56$ ) show phase transitions from the cubic (NaCl) room-temperature phase to noncubic low-temperature phases.<sup>1,2</sup> The low-temperature state of the Br-rich crystals is regarded as glasslike with an average cubic lattice and frozen-in CN orientations and a distribution of inhomogeneous strains.<sup>3-5</sup> The two types of low-temperature states are announced by a softening of the elastic shear constant  $C_{44}$  of the cubic phase.<sup>6,7</sup>

The structural phase transition of pure KCN at  $T_s = 168$  K is of first order. As the CN concentration  $x$  is reduced,  $T_s(x)$  and the jump of the order parameter at  $T_s(x)$  decrease.<sup>2</sup> For  $x=0.65$  and  $0.70$  the x-ray powder diffraction patterns show two subsequent transitions from cubic to rhombohedral and further to monoclinic.<sup>2</sup> The splitting of the cubic (222) powder line of the present sample is shown in Fig. 1. The data suggest that the transitions are continuous with the cubic-to-rhombohedral transition at  $T_s = (111.7 \pm 0.4)$  K. The relative change of the cell volume at  $T_s$ , if there is any, is less than 0.001.

Cowley<sup>8</sup> and Folk, Iro, and Schwabl<sup>9</sup> have treated the ferroelastic transitions with renormalization-group theory and predict unusual properties for the universality class  $m=2$  for which the present crystal appears to be a first example: In ferroelastic transitions the primary order parameter is a homogeneous strain and the conjugate fluctuations are long-wavelength acoustic phonons.  $m$  denotes the dimension of the subspace of reciprocal space which is covered by the fluctuations. With our concentration on cubic crystals the class  $m=0$  corresponds to isomorphic transitions with a volume collapse at  $T_s$  and a soft elastic constant  $A_{1g}$ , as observed, e.g., in Ce metal. Cubic-to-tetragonal transitions belong to the class  $m=1$ . The fluctuations

are  $E_g$  phonon modes, which propagate along the face diagonals. A prominent example is  $\text{Nb}_3\text{Sn}$ .  $m=0$  and  $m=1$  systems are well described by mean-field theories. For  $m=2$  the order parameter is a spontaneous shear. The transition involves a softening of the elastic shear constant  $C_{44}$  and leads to diverging critical fluctuations of  $T_{2g}$  symmetry, the wave vectors of which lie in the cubic planes. The upper critical dimension for this class is three, and hence one expects logarithmic corrections to the mean-field behavior in a three-dimensional crystal. A consequence of the softening of the  $T_{2g}$  phonons is the divergence of the mean-square displacement  $\langle u^2 \rangle$  at  $T_s$ . Thus the system should pass through a state of lost crystalline order when transforming from the high- to low-temperature crystalline phase. Folk, Iro, and Schwabl<sup>9</sup>

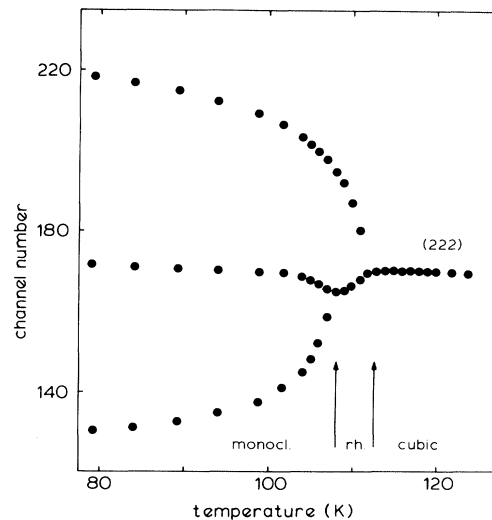


FIG. 1. The splitting of the (222) x-ray powder line upon the two consecutive transitions cubic to rhombohedral to monoclinic. The channel number is a linear measure of the Bragg angle.

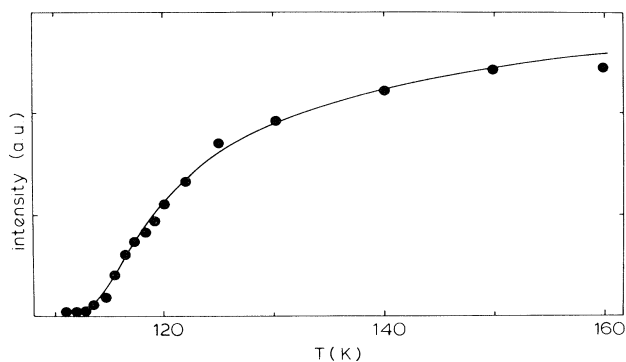


FIG. 2. The temperature dependence of the (620) Bragg intensity of the x-ray experiment. The solid line is calculated from  $C_{44}(T)$ .

have noted a “conspicuous” absence of  $m = 2$  systems in nature.

We will present x-ray, ultrasonic, and inelastic-neutron-scattering results on the cubic phase ( $x = 0.73$ ). X-ray diffraction on the single crystal shows a dramatic decrease of the intensities of the Bragg reflections with decreasing  $T$ . For Fig. 2 the profiles of  $(6, 2, 0) \pm (0, \xi, 0)$  scans were analyzed in terms of a superposition of a Gaussian peak representing the Bragg component and of a Lorentzian peak representing the thermal diffuse intensity.

The  $T$  dependence of the Gaussian intensity is shown in the figure. At 114 K the (620) Bragg peak has dropped to 3% of the high-temperature intensity. When interpreted as a Debye-Waller factor this value corresponds to an rms displacement of 11% of the next-neighbor distance.

The ultrasonic experiments, carried out with 10-MHz transducers and use of the pulse-echo overlap method, gave clear signals down to 135 K. At this temperature the last echo disappeared.  $C_{44}(T)$  is shown in Fig. 3. The usual mean-field  $T$  dependence of the form<sup>6,10</sup>  $C_{44} = C_{44}^0 (T - T_0)/(T - T_a)$  was fitted to the data, yielding  $T_0 = 123$  K,  $T_a = -130$  K, and  $C_{44}^0 = 5.4 \times 10^{10}$  dyn/cm<sup>2</sup> (dashed line). Note that the extrapolated ordering temperature  $T_0$  lies well above the actual transition temperature  $T_s$ .

For a closer inspection of the elastic response neutron experiments have been carried out in the triple-axis spectrometer TAS7 at the Risø National Laboratory with use of a fixed outgoing neutron energy of 2.5 meV, Be filters before and after the sample, and a collimation of 60'-60'-60'-60' along the beam path. The energy resolution was 40  $\mu$ eV at zero energy transfer. Series of constant- $Q$  scans,  $Q = (1, 1, 1) + (\xi, 0, 0)$ ,  $0.03 \leq \xi \leq 0.10$ , have been performed at several temperatures between 171 and 112.3 K. This scattering geometry measures the  $T_{2g}$  transverse acoustic phonons with sound velocity proportional to  $C_{44}$ . As  $T_s$  is

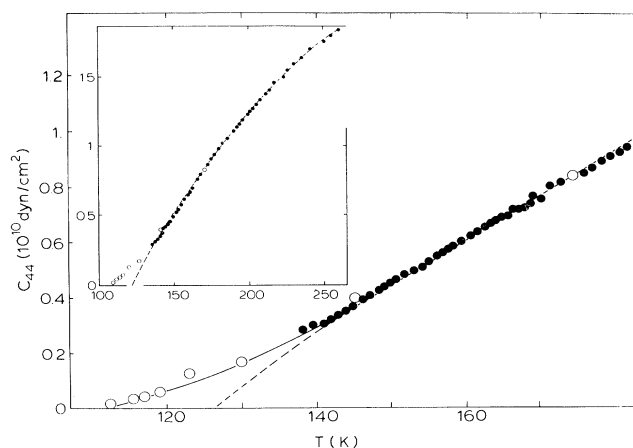


FIG. 3. The temperature dependence of the elastic shear constant  $C_{44}$  (ultrasonics, solid circles; inelastic neutron scattering, open circles). The dashed line is a best fit with an overall mean-field behavior; the solid line shows the renormalization-group prediction.

approached the phonon frequencies decrease and the central peak grows (Fig. 4). At higher temperatures where clear phonon sidebands have been observed, the width of the phonon signals increases with  $\xi$ , and

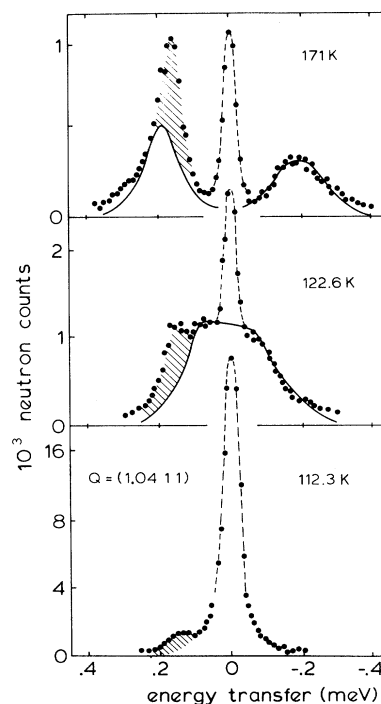


FIG. 4. Profiles of constant- $Q$  scans of the inelastic-neutron-scattering experiment. The solid line is the fit of the model, which is described in the text, to the phonon sidebands. The hatched excess intensity is picked up from the (111) Bragg peak as a result of the finite resolution.

at  $\xi = 0.10$  a crossover from fast to slow relaxation is approached (see below). At the lowest temperature, 112.3 K, the scan profiles at all  $\xi$  investigated consist of a single peak at zero energy.

For a parametrization of these results we used the following mean-field phonon susceptibility<sup>11</sup>  $D(q, \omega)$  which assumes a bilinear coupling between the phonons and a relaxational-type orientational susceptibility  $\chi_R$ :

$$D(q, \omega) = 2\omega_0 / (\omega_0^2 - \omega^2 - g^2\omega_0^2\chi_R), \quad (1)$$

$$\chi_R^{-1} = (T - T_a) \left( 1 + \frac{T}{T - T_a} \frac{i\omega}{\Gamma} \right).$$

$\omega_0$  is the frequency of phonons decoupled from the CN orientations,  $g^2$  is the coupling coefficient, and  $\Gamma$  is the orientational relaxation rate. Equation (1) has given an adequate description of the elastic response of several cyanides.<sup>12</sup> It includes the limits of slow and fast relaxation, depending upon whether the phonon frequency is smaller or larger than  $\Gamma$ . In the long-wavelength limit it predicts a soft-mode behavior of the acoustic phonons, i.e., the elastic shear constant of the form given above. The elastic response vanishes at  $T_0$ ,  $T_0 = g^2 + T_a$ . There are four parameters only, apart from a scale factor:  $T_a$ ,  $g^2$ ,  $\Gamma$ , and  $C_{44}^0$ . Theoretical scan profiles have been calculated from  $D(q, \omega)$  with consideration of the experimental resolution (solid lines of Fig. 4). The parameters are listed in Table I, where each set of parameters results from simultaneous fits of the series of constant- $Q$  scans with different  $\xi$  values at a given  $T$ . The parameters describe the case of fast relaxation, a case in which Eq. (1) does not supply a central peak.<sup>12</sup> The central peak is a feature beyond the present mean-field expression.

Deviation from the mean-field  $T$  dependence of  $C_{44}$  shows up as a  $T$  dependence of the temperature  $T_0$ . The  $T$  dependence of the scale factor signals a transfer of scattered intensity from the phonon sidebands to the central peak. At the lowest temperatures the basis for the fit is of course poor; nevertheless the fit gives a feeling for the upper limits of the phonon frequencies. The neutron results on  $C_{44}$  as calculated from  $C_{44}^0$  and  $g^2$  are included in Fig. 3.

As an alternative to Eq. (1) we tried fits by expressions of the type which have been used to describe the elastic response in substances like  $\text{Nb}_3\text{Sn}$  with phonon sidebands and a central peak<sup>13,14</sup> at the expense of at least two additional parameters compared to Eq. (1). It is obvious that a reliable determination of such a large number of parameters is not feasible in the low- $T$  regime, so that we finally returned to Eq. (1). Apart from this practical reason we think that Eq. (1) is based on a physical background which should not be abandoned.

TABLE I. Results of the fit of Eq. (1) to the profiles of the neutron scans.  $C_{44}^0$  and  $T_a$  have been held constant at the values determined from the ultrasonic experiment. The scale factor,  $T_0$  for  $T \geq 155$  K, and  $\Gamma$  for  $T \geq 130$  K have been treated as free parameters.  $C_{44}$  is calculated from  $C_{44} = C_{44}^0 (T - T_0) / (T - T_a)$ .

$T$ (K)	$T_0$ (K)	$\Gamma$ (meV)	Scale (arbitrary units)	$C_{44}$ ( $10^{10}$ dyn/cm <sup>2</sup> )
171	123	1.5	1.4	0.85
146	123	1.5	1.4	0.42
130	121	1.5	1.2	0.18
122.6	117	1.5	0.9	0.13
119	116	1.5	0.7	0.06
115	113	1.5	0.5	0.04
112.3	111.7	1.5	0.3	0.01

The deviations from the mean-field  $T$  dependence of  $C_{44}$  and the Bragg intensity are clearly apparent in Figs. 2 and 3. This unusual behavior is well accounted for by the renormalization-group predictions<sup>9</sup> (solid lines in these figures):  $C_{44} \sim \tilde{\tau}$  and  $\langle u^2 \rangle \sim \tilde{\tau}^{-1}$  with  $\tilde{\tau} = \tau / |\ln \tau|^{1/3}$ ,  $\tau = T/T_s - 1$ . In the calculation of the Bragg intensities it turns out that the effect of the small  $T$  dependence of the other elastic constants,  $C_{11}$  and  $C_{12}$ , is negligible.

As mentioned in the introduction, the critical behavior of an  $m = 2$  system should eventually lead—when some threshold for  $\langle u^2 \rangle$  is reached—to a breakdown of the concept of a crystal lattice with one-phonon modes as dominant excitations. In fact there is experimental evidence that at temperatures close to  $T_s$  the present system is on the verge of “melting” and behaves to some degree like a system at the lower critical dimension: The rms displacements fulfill the Lindemann criterion for melting. Within the experimental resolution the elastic shear constant vanishes. In addition to the soft-phonon modes, quasistatic disorder scattering, the central peak, is observed which we interpret as the manifestation of random strain fields; i.e., its intensity is a measure of to what extent the crystalline order is violated. We note that the existence of random strain fields in the mixed cyanides is a consequence of the effective strain-mediated CN-CN interaction.<sup>3,15</sup> From the experimental data one cannot decide whether the central peak or the soft-phonon response diverges at  $T_s$ , but from the mere fact that the sample finally transforms into a crystalline low-temperature phase we conclude that the transition is ultimately driven by soft lattice modes in the presence of noncritical random strains.

The mention of random strain fields raises the question of whether the theory of  $m = 2$  systems, which has been developed for pure systems only, is valid for the present mixed crystals. Random fields should un-

doubtedly modify the critical behavior or even suppress it completely. We note that our results bear a great resemblance to the elastic response functions calculated by Halperin and Varma<sup>14</sup> for structural phase transitions in the presence of various types of defects. Finally the formation of the glasslike state at slightly lower CN concentrations than the present one ( $x < 0.56$ ) is a clear demonstration that CN groups fixed in orientation can even destroy long-range order and thus prevent the system from transforming into a non-cubic crystalline low-temperature phase.

Summarizing, we have found that the cubic-rhombohedral ferroelastic transition in  $(\text{KBr})_{0.27}(\text{KCN})_{0.73}$  appears to be continuous and that it involves a complete softening of the elastic constant  $C_{44}$ . Within the concept of a "virtual crystal" this implies that the system belongs to the  $m = 2$  universality class for ferroelastic transitions and it represents the first example of this kind. On the other hand, random strains as a consequence of the orientational-translational coupling in combination with the non-stoichiometric nature of a mixed crystal definitely play an important role in the critical behavior which we suggest should be studied theoretically.

We thank Professor Haussühl, who generously supplied the sample.

<sup>1</sup>J. M. Rowe, J. J. Rush, and S. Susman, Phys. Rev. B **28**, 3506 (1983).

<sup>2</sup>K. Knorr and A. Loidl, Phys. Rev. B **31**, 5387 (1985).

<sup>3</sup>J. M. Rowe, J. J. Rush, D. G. Hinks, and S. Susman, Phys. Rev. Lett. **43**, 1158 (1979); K. H. Michel and J. M. Rowe, Phys. Rev. B **22**, 1417 (1980).

<sup>4</sup>A. Loidl, R. Feile, and K. Knorr, Phys. Rev. Lett. **48**, 1263 (1982).

<sup>5</sup>A. Loidl, M. Müller, G. McIntyre, K. Knorr, and H. Jex, Solid State Commun. **54**, 367 (1985).

<sup>6</sup>R. Feile, A. Loidl, and K. Knorr, Phys. Rev. B **26**, 6875 (1982).

<sup>7</sup>C. W. Garland, J. Z. Kwiecien, and J. C. Damien, Phys. Rev. B **25**, 5818 (1982).

<sup>8</sup>R. A. Cowley, Phys. Rev. B **13**, 4877 (1976).

<sup>9</sup>R. Folk, H. Iro, and F. Schwabl, Z. Phys. B **25**, 69 (1976), and Phys. Rev. B **20**, 1229 (1979).

<sup>10</sup>W. Rehwald, J. R. Sandercock, and M. Rossinelli, Phys. Status Solidi (a) **42**, 699 (1977).

<sup>11</sup>B. D. Silverman, Phys. Rev. Lett. **25**, 107 (1970).

<sup>12</sup>A. Loidl, R. Feile, K. Knorr, and J. K. Kjems, Phys. Rev. B **29**, 6052 (1984).

<sup>13</sup>G. Shirane and J. D. Axe, Phys. Rev. Lett. **27**, 1803 (1971).

<sup>14</sup>B. I. Halperin and C. M. Varma, Phys. Rev. B **14**, 4030 (1976).

<sup>15</sup>B. de Raedt, K. Binder, and K. H. Michel, J. Chem. Phys. **75**, 2977 (1981).